MULTIBAND FRACTAL PLANAR INVERTED F ANTENNA (F-PIFA) FOR MOBILE PHONE APPLICATION

N. A. Saidatul, A. A. H. Azremi, R. B. Ahmad, P. J. Soh and F. Malek

School of Computer and Communication Engineering
University Malaysia Perlis (UniMAP)
Kangar, Perlis, Malaysia

Abstract—The design of a novel Fractal planar inverted F antenna (F-PIFA) based on the self affinity property is presented in this paper. The procedure for designing a Fractal Planar Inverted F Antenna is explained and three different iterations are designed for use in cellular phones. The F-PIFA has a total dimension of $27\,\mathrm{mm} \times 27\,\mathrm{mm}$ and has been optimized to be operational at GSM (Global System for Mobile Communication), UMTS (Universal Mobile Telecommunication System) and HiperLAN (High Performance Radio LAN) with the frequencies range from 1900 MHz to 2100 MHz, 1885 to 2200 MHz and 4800 MHz to 5800 MHz respectively. The antenna achieved $-6\,\mathrm{dB}$ return loss at the required GSM, UMTS and HiperLan frequencies with and has almost omnidirectional radiation pattern. This antenna has been tested using realistic mobile phone model and has met the performance criteria for a mobile phone application. Simple semi-empirical formulas of the operational frequency, numerical calculation and computational SAR of the antenna also has been presented and discussed.

1. INTRODUCTION

The demands on mobile phone performance have increased rapidly over the last few years. The economics of manufacture makes it very desirable to make handsets that cover several of the increasing number of world frequency bands. For high end products both economics and user expectations require them to cover as many bands as possible.

Corresponding author: N. A. Saidatul (s0730810155@student.unimap.edu.my).

Currently at least five bands are assigned for world wide mobile services (850, 900, 1800, 1900 and 2100 MHz) so many antennas must cover 824–960 MHz and 1710–2170 MHz with high efficiency. Not only must the bandwidth of the antenna be very wide, but when transmitting data using high order modulation schemes [1], it is very important that handset antenna gain and efficiency are high as possible. Nowadays mobile phone has the Bluetooth and Wireless LAN capability. By adding Bluetooth or WLAN at the mobile phone, data transfer can be easily made. For Bluetooth or WLAN Communication System uses frequency range from 2400–2450 MHz, hence the antenna designed must be able to operate in this frequency range.

The Planar inverted-F antenna (PIFA) is currently being used as an embedded antenna in many radiotelephone handsets [2–10]. It is one of the most promising antenna types because it is small and has a low profile, making it suitable for mounting on portable equipment. The planar inverted-F antenna is a microstrip antenna design shows much promise in dealing with the shortfalls of the $\lambda/4$ monopole antenna in mobile communication applications [11, 12]. The antenna also has a high degree of sensitivity to both vertically and horizontally polarized radio waves, thus making the Planar Inverted-F Antenna ideally suited to mobile applications. In addition, PIFAs can reduce the possible electromagnetic energy absorption by the mobile handset user's head, because of relatively smaller backward radiation toward the user. This antenna also is reasonably efficient and free of excessive radiation illuminating the user's head (low SAR value) [13–18].

However, PIFA have some drawback s such as low efficiency, narrow bandwidth and not multiband. To enhance these drawbacks, especially narrow bandwidth, and to meet the miniaturization requirements of mobile units, Fractal PIFA has been design to achieve the design of internal compact and broadband microstrip patch antennas. Fractal antennas are comprised of elements patterned after self-similar designs to maximize the length, or increase the perimeter [19]. The beneficial give useful applications in cellular telephone and microwave communications. Furthermore, it is found a little adjustment of the shape can make it work in the demanded resonant frequencies [20]. At present time, there is no research on the combination of fractal to PIFA topology. Therefore, this paper proposed PIFA fractals which can be used as an internal antenna solution and to produce a wideband frequency. The proposed designs are able to provide coverage at all desired frequency bands [21–24]. In order to obtain a good fundamental antenna design, the initial studies were carried out theoretically, using CST Microwave Studio simulation software.

2. ANTENNA DESIGN

As mobile phones are becoming smaller with time, it is not feasible for separate antenna element to be used to facilitate multiband operations. This proposes a novel design in that a Fractal antenna as the patch for PIFA is directly connected with a feed strip and positioned at a plane perpendicular to a ground plane. The antennas are design using CST Studio Suit 2008 software. The essential parameter specifications for the design of the rectangular planar inverted F antenna are as in Table 1.

Table 1. Design parameter specifications of Planar Inverted F Antenna (PIFA).

Shape	Rectangular
Frequency of operation	GSM 1800 (1710–1880 MHz) 3G-UMTS2000 (1885–2200 MHz) WLAN (2400–2483 MHz) HiperLAN (4800–5800 MHz)
Dielectric constant of the substrate	3.38 (Rogers RO4003C)
Height of dielectric substrate	0.813 mm
Feeding Method	probe feed
VSWR	2 : 1
Gain	0 dB–4 dB
SAR	$< 2\,\text{W/kg}$ at 2000 MHz

3. DESIGN PROCEDURE

The configuration of the proposed PIFA is shown in Figure 1. The rectangular radiating patch is printed on rogers board (Rogers, RO4003C) with epsilon 3.38, has dimensions $L_1 \times L_2$; and is located in the middle of a 0.5 mm thick copper plate ground plane with dimensions $L_g \times W_g$. The antenna height h is filled with an air substrate ($\varepsilon_r = 1.0$). The shorting plate consists of a vertical conducting strip and it is used not only to connect between the patch and ground, but also to support the whole antenna. The 50 Ω coaxial probe has a radius of 0.5 mm and is fed in the centre line of the rectangular patch. The distance between the feeding position and the shorting plate varies

depends on the fractal's iterations. The coaxial feed excites the PIFA's TM_{10} mode.

The operating frequency of a microstrip patch antenna is inversely proportional to its physical dimensions. For a standard, coax-fed, quarter-wave microstrip patch antenna, the operating frequency can be approximately determined from the length of antenna patch as follows:

$$L_1 \approx \frac{\lambda_d}{4} = \frac{1}{4} \cdot \frac{c}{f\sqrt{\varepsilon_r}} \tag{1}$$

$$L_2 = \frac{c}{4f}\sqrt{\frac{2}{\varepsilon_r + 1}} \tag{2}$$

Or the above equation can be use to fine the total length,

$$f = \frac{c}{4(L_1 + L_2)} \tag{3}$$

where λ_d is the wavelength inside the substrate. The lengths L_1 and the width L_2 can be subsequently optimize to obtain an improved frequency match by do optimization procedure through experimental trials. One method of reducing PIFA size is simply by shortening the antenna by adding a shorting pin. Though, this approach affects the impedance at the antenna terminals such that the radiation resistance becomes reactive as well. This can be compensated with capacitive top loading. In practice, the missing antenna height is replaced with an equivalent circuit, which improves the impedance match and the efficiency.

3.1. PIFA Design Calculation

In designing a Fractal PIFA, the following formulas were implemented as an outline in designing procedures. The width and the length, L_1 and L_2 of the patch that can be calculated as [4],

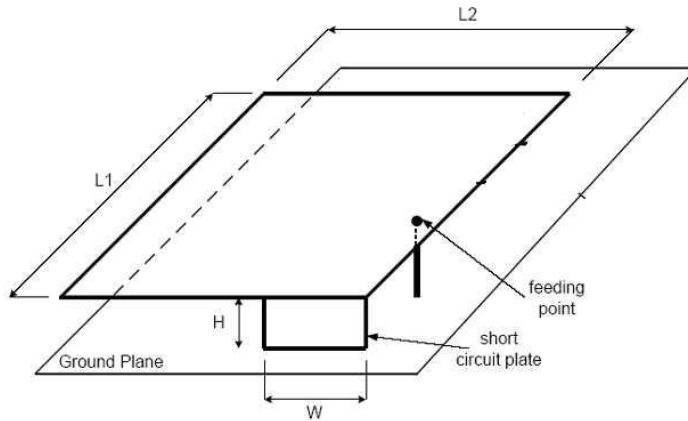$$f = \frac{1}{4}\left(\frac{c}{L_1 + L_2}\right) \tag{4}$$

where,

$c = $ free space velocity of light, $3 \times 108\,\text{m/s}$
$f = $ frequency of operation
$(L_1 + L_2) = x \qquad x = $ total length
$x = \dfrac{c}{4f} = \dfrac{3 \times 10^8}{4\,(2\,\text{GHz})} = 37.5\,\text{mm}$

Figure 1. Geometry of the proposed PIFA.

$$\therefore (L_1 + L_2) = 37.5 \, \text{mm} \qquad L_1 \approx L_2 \approx 18.8 \, \text{mm}$$
after optimized;
$$L_1 = L_2 = 27 \, \text{mm}$$

This equation is been used to determine the all necessary dimensions of the microstrip patch antenna. The most significant parameters required for the design of this antenna are the width and length (L_1 and L_2) of the patch antenna. The results are very sensitive to changes in both L_1 and L_2. The value after the calculations is used as the initial value, but during optimization using CST Studio Suit 2008 software, some of the value been attuned according to the simulation result to obtain the desired frequency.

3.2. Fractal's Design

For design of quadrate rectangular fractal antenna, a two-dimension triadic Cantor array is used as generating element:

$$\begin{matrix} 1 & 1 & 1 \\ 1 & 0 & 1 \\ 1 & 1 & 1 \end{matrix}$$

Then rectangular fractal antenna array is constructed recursively by replacing of 1 by whole base element and rectangular antenna of corresponding order. The antenna array factor for the rectangular fractal antenna for distance between elements of the antenna $d_x =$

$d_y = \lambda/2$ is [6]:

$$A_{f\,\text{norm}} = 4^{-p} \prod_{p=1}^{p} \left[\cos\left(3^{p-1}\pi u_x\right) + \cos\left(3^{p-1}\pi u_y\right)\right]$$
$$+ \left[2\cos\left(3^{p-1}\pi u_x\right) + \cos\left(3^{p-1}\pi u_y\right)\right]$$

where

$$\begin{cases} u_x = \sin\theta\cos\varphi - \sin\theta_0\cos\varphi_0 \\ u_y = \sin\theta\sin\varphi - \sin\theta_0\sin\varphi_0 \end{cases}$$

In order to start designing rectangular type of fractal antenna, a large square structure is created in the plane and divided into nine smaller congruent squares where the open central square is dropped out. The remaining eight square are divided into nine smaller congruent squares with again each central is dropped out. We continue this process infinitely often obtaining a limiting configuration which can be seen as a generalization of the Cantor set. Let N_n be the number of black boxes, L_n is the scale factor for length of a side of white boxes, A_n is the scale factor for fractional area of black boxes after the nth iteration.

$$N_n = 8^n \tag{5}$$

$$L_n = \left(\frac{1}{3}\right)^n \tag{6}$$

$$A_n = L_n^2 N_n = \left(\frac{8}{9}\right)^n \tag{7}$$

The ideal fractal antenna is obtained by iterating infinite number of times. However, in order to create practical antennas only a few iterations are used. Figure 2 show the process of iteration for Fractal design. The Fractal design is printed over a thin Rogers 4003 substrate of dielectric constant $\varepsilon_r = 0.813$ with thickness $= 0.813\,\text{mm}$.

3.3. First Iteration of Fractal PIFA

The first iteration structure designed by divided this square into 9 smaller square and removed the square at the center as the remaining square is 8. The length, L_1 is the length scale factor for first iteration, 0.333 multiply with 27 mm, get the length for Small Square is 9 mm. For basic square patch antenna the area is 27×27 mm, $A_0 = 729\,\text{mm}^2$. After first iteration the total area become $= 648\,\text{mm}^2$. Area for small square is $81\,\text{mm}^2$. The A_1 is the scale factor for the fractional area after first iteration.
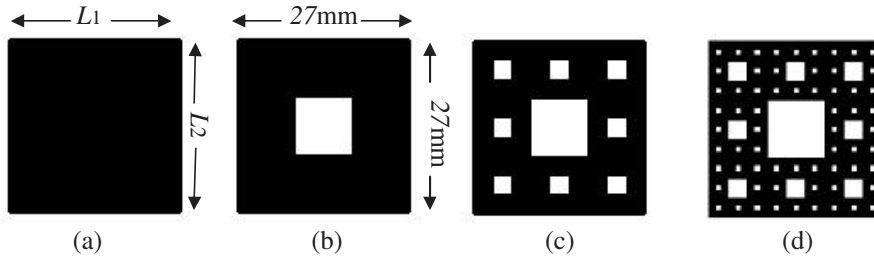
Figure 2. Dimension for Fractal PIFA. (a) 0 Iteration, (b) 1st Iteration, (b) 2nd Iteration, (c) 3rd Iteration.

3.4. Second Iteration of Fractal PIFA

The second iteration fractal PIFA structure was designed by divided each remaining eight squares into nine smaller square. Then drop the entire center square for each remaining square. The remaining

Table 2. Calculation for each iteration of F-PIFA.

First Iteration	Second Iteration	Third Iteration
$Area_1 = 729\,\text{mm}^2 - 81\,\text{mm}^2$ $= 648\,\text{mm}^2$	$Area_2 = Area_1 - 72\,\text{mm}^2$ $= 648\,\text{mm}^2 - 72\,\text{mm}^2$ $= 576\,\text{mm}^2$	$Area_3 = Area_2 - 64\,\text{mm}^2$ $= 576\,\text{mm}^2 - 64\,\text{mm}^2$ $= 512\,\text{mm}^2$
$A_1 = \dfrac{Area_1}{A_0}$ $= \dfrac{648\,\text{mm}^2}{729\,\text{mm}^2}$ $= 0.888$	$A_2 = \dfrac{Area_2}{A_0}$ $= \dfrac{576\,\text{mm}^2}{729\,\text{mm}^2}$ $= 0.790$	$A_3 = \dfrac{Area_3}{A_0}$ $= \dfrac{512\,\text{mm}^2}{729\,\text{mm}^2}$ $= 0.702$
The equation above can simplified it by using the Equation (7) $N_1 = 8^1$ $L_1 = \left(\dfrac{1}{3}\right)^1$ $= 0.333$ $0.333 \times 27\,\text{mm} = 8.991\,\text{mm}$ $\therefore 9\,\text{mm} \approx$ length for Small Square	$N_2 = 8^2$ $L_2 = \left(\dfrac{1}{3}\right)^2$ $= 0.111$ $0.111 \times 27\,\text{mm} = 3\,\text{mm}$ $\therefore 3\,\text{mm} \approx$ length for Small Square	$N_3 = 8^3$ $L_3 = \left(\dfrac{1}{3}\right)^2$ $= 0.037$ $0.037 \times 27\,\text{mm} = 1\,\text{mm}$ $\therefore 1\,\text{mm} \approx$ length for Small Square

smaller square for this stage is 64. L_2 is the length scale factor for second iteration, 0.111 multiply with 27 mm, get the length for Small Square is 3. The A_2 is the scale factor for the fractional area after first iteration. After second iteration the total area become 576 mm^2. Area for one small square is 9 mm^2 and the total area for small square that has been removed is 72 mm^2.

3.5. Third Iteration of Fractal PIFA

The third iteration fractal PIFA structure was designed by divided each remaining 64 squares into nine smaller square. The entire center square for each remaining square being omitted. The remaining smaller square for this stage is N_3, 512. L_3 is the scale factor for third iteration, 0.037 multiply with 27 mm, get the length for Small Square is 1. After third iteration the total area become 512 mm^2. Area for one small square is 1 mm^2 and the total area for small square that has been removed is 64 mm^2. All the calculation is state in Table 2 down below.

3.6. Feeding Technique

The feed point must be located at a point on the patch, where the input impedance is 50 ohms for the resonant frequency. 50 ohms is a great compromise between power handling and low loss, for air-dielectric coax. For different locations of the feed point, the return loss (RL) is compared and that feed point is selected where the RL is most negative. Matching is usually required between the feed line and an antenna. This is because the antenna input impedances differ from customary $50\,\Omega$ line impedance. Matching may be achieved by properly selecting the location of the feed line. Since probe feed method is used, therefore some parameters must be calculated. The matching impedance used was $50\,\Omega$. To match this impedance, the connector must be place at a distance from the edge that matches $50\,\Omega$. Equations (8) through (11) below were used to calculate the exact position to place a port and the computation is shown in Table 3.

$$\lambda_o \approx \frac{c}{f_r} \tag{8}$$

the wave number,

$$G_1 = \frac{w}{120(\lambda_o)}\left[1 - 2\left(\frac{1}{24}\right)(k)^2\right] \tag{9}$$

$$Z_{in} = \frac{1}{G_1} \tag{10}$$

$$R_{in} = \cos^{-1}\left(\sqrt{\frac{Z_o}{Z_{in}}}\right) x \frac{l}{\pi} \qquad (11)$$

Determination of feed point location;

$$\lambda_o \approx \frac{c}{f_r}$$

where
$$w \text{ and } l = 27\,\text{mm} \qquad k = 1.380658^{-23}.$$

4. THE ANTENNA RESULT AND DISCUSSION

As illustrated from the Figure 3, simulated and measured result according to $-9.8\,\text{dB}$ (VSWR $2:1$) the bandwidth of the antenna for 0 iteration is $850\,\text{MHz}$ (1700–$2550\,\text{MHz}$), while for 1st iteration

Table 3. Calculation of feed point location at $2.0\,\text{GHz}$ and $5.0\,\text{GHz}$.

Frequency	2.0 GHz, $\lambda_o = 0.15$	5.0 GHz, $\lambda_o = 0.06$
G_1	$= \frac{w}{120(\lambda_o)}\left[1 - 2\left(\frac{1}{24}\right)(k)^2\right]$ $= \frac{27\,\text{mm}}{120(0.15)}\left[1 - 2\left(\frac{1}{24}\right)(1.380658^{-23})^2\right]$ $= 1.5\,\text{m}$	$= \frac{w}{120(\lambda_o)}\left[1 - 2\left(\frac{1}{24}\right)(k)^2\right]$ $= \frac{27\,\text{mm}}{120(0.06)}\left[1 - 2\left(\frac{1}{24}\right)(1.380658^{-23})^2\right]$ $= 3.75\,\text{mm}$
Z_{in}	$= \frac{1}{G_1}$ $= \frac{1}{1.5\,\text{mm}}$ $= 666.66$	$= \frac{1}{G_1}$ $= \frac{1}{3.75\,\text{mm}}$ $= 266.66$
R_{in}	$= \cos^{-1}\left(\sqrt{\frac{Z_o}{Z_{in}}}\right) \times \frac{l}{\pi}$ $= \cos^{-1}\left(\sqrt{\frac{50}{666.66}}\right) \times \frac{27\,\text{mm}}{\pi}$ $= 12.85\,\text{mm}$	$= \cos^{-1}\left(\sqrt{\frac{Z_o}{Z_{in}}}\right) \times \frac{l}{\pi}$ $= \cos^{-1}\left(\sqrt{\frac{50}{266.66}}\right) \times \frac{27\,\text{mm}}{\pi}$ $= 9.651\,\text{mm}$
Optimized value	$R_{in} = 12.6\,\text{mm}$	$R_{in} = 8.5\,\text{mm}$

is 940 MHz (1770–2710 MHz), 2nd iteration are 590 MHz (1630–
2220 MHz) at the lower band and 1520 MHZ (4780–5300 MHz) at the
upper band respectively as well as for 3rd iteration are 500 MHz (1700–
2200 MHz) at the lower band and 400 MHz (4830–5230 MHz) for the

Table 4. S_{11} result for measured and simulated F-PIFA.

F-PIFA	OPERATING FREQUENCY	FREQUENCY BAND (MHz)	BANDWIDTH (MHz)
0 Iteration	2 GHz	1700–2550	850 (42.5%)
1st Iteration	2 GHz	1770–2710	940 (47%)
2nd Iteration	2GHz	1630–2220	590 (29.5%)
	5GHz	4780–5300	520 (10.4%)
3rd Iteration	2 GHz	1700–2200	500 (25%)
	5 GHz	4830–5230	400 (8%)

(a) 0 Iteration

(b) 1st Iteration

(c) 2nd Iteration
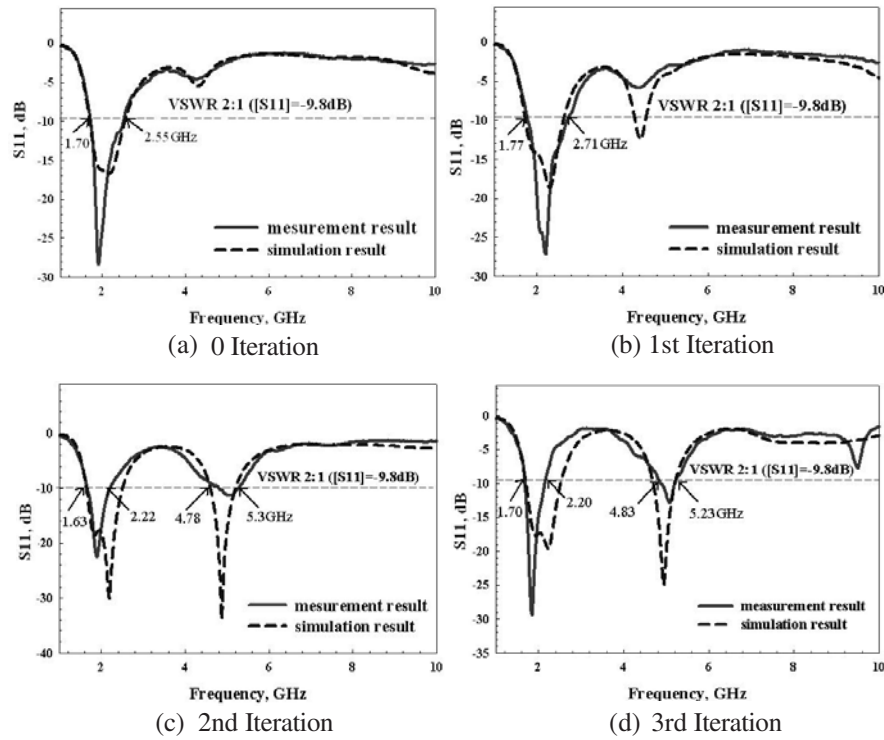
(d) 3rd Iteration

**Figure 3.** The simulated and measured S_{11} result of the designed
antenna.

upper band. This result can be seen in Table 4. It is very clear to observe that, 1st iteration produce a wider bandwidth compare to the others iterations so the antenna has the capacity to cover GSM 1800, GSM 1900, UMTS 2000, and Bluetooth 2450 bands as shown in Figure 3(b). As the iteration increase, the bandwidth narrower but generates another resonant frequency at 5 GHz. But only 2nd iteration accomplishes the bandwidth for 3G UMTS and hiperLAN. Thus, the F-PIFA stops increasing the iteration and start to study the behavior of F-PIFA at 2nd iteration.

4.1. PIFA as Internal Antenna for Mobile Phone

After the antenna design is completed, the next step is to evaluate the designed antenna performance in a complete phone model. This enable the evaluation of the coupling effects of neighboring object such as the battery, camera, as well as the influence of dielectric materials such as the housing and display screen. The Fractal Planar Inverted F Antenna was integrated and positioned at the space provided in mobile phone circuit as shown in Figure 4. An additional parasitic element is added to alleviate the low band frequency, thus generate the 900 MHz resonant. The 2 mm × 60 mm strip of copper plate is added in front of the F-PIFA, consequently creating capacitive load and the frequency shift downward, however a new frequency has been created which is the low resonant.
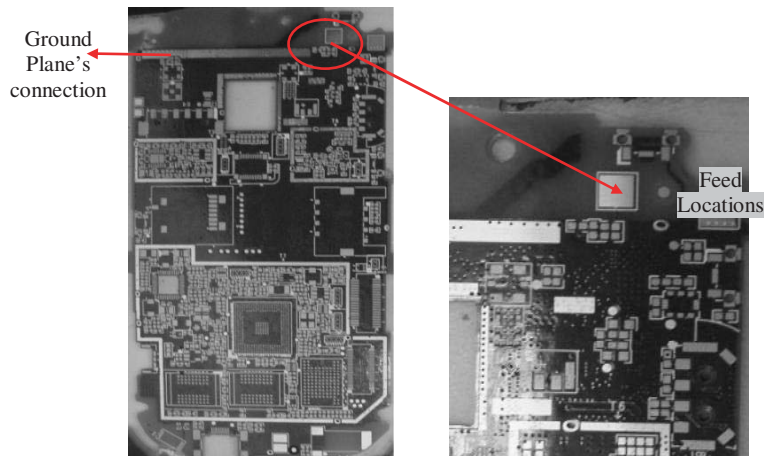
Figure 4. Actual PCB size for candy bar phone and the antenna feed and ground plane location.
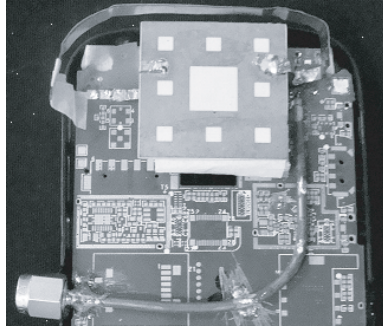
Figure 5. F-PIFA mounted on the candy bar phone.

(a)   (b)
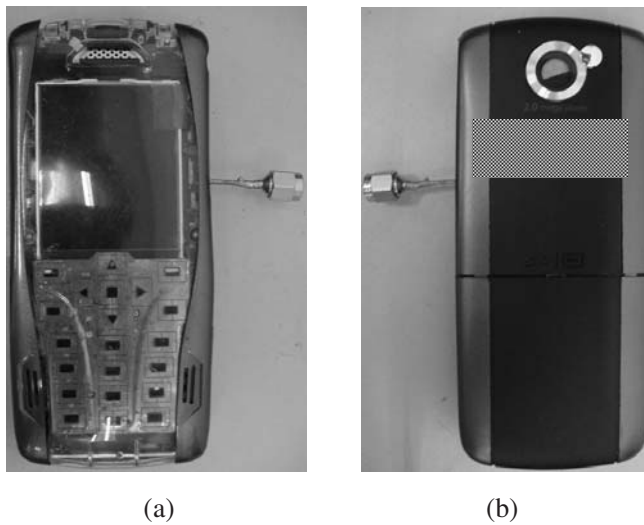
Figure 6. F-PIFA in full phone model. (a) Front view of the phone model. (b) Rear view of the phone model.

The antenna is connected to the phone model via a vertical shorting strip and is fed via a feed strip connected to a $50\,\Omega$ transmission line etched on the left as shown in Figure 5. The cellular system currently operates at number of frequency bands, 900 MHz, 1800 MHz, and 2000 MHz. The new Fractal Planar Inverted F Antenna covers the GSM (800, 900, 1800 and 1900 MHz), along with Wireless LAN 2400 MHz for 802.11b and g standards and 5000 MHz for 802.11a standard.

As shown in Figure 6 is the mobile phone model with the Fractal Planar Inverted F Antenna inside. The plastic housing will lower the resonance due dielectric loading, thus the antenna has to attune hence to get the correct resonance. Housing covering the antenna must not be metal or metallic coated because it will drastically influence the antenna performance. The antenna been measured using the actual housing, with battery, shield cans, speaker and camera for antenna verification.

Figure 7 indicate the S_{11} result for the F-PIFA with and without the full phone model. As can be examined, when the antenna is cover with the mobile phone, the resonance shifted to the left. Therefore, the antenna length needs to be cut slightly to move the resonance up until it resonate at the correct band. The changing resonant can be observed using network analyzer. This is the way to optimize the antenna.

In Figure 8 indicate the result for efficiency and gain. Based on the result, this antenna is convincing to be used as internal antenna for mobile communication. Even though, the result measurement with and without the full phone has a slightly difference, but this result is still acceptable due to the different is less than 10%. As can be seen, the antenna radiation efficiency with full phone model is still more than 50%. In Figure 9 show the position of the antenna during the measurement in the anechoic chamber. In Figure 10 indicate the 2D and 3D radiation pattern of the phone with and without head phantom. The radiation pattern is obviously influenced by the head.

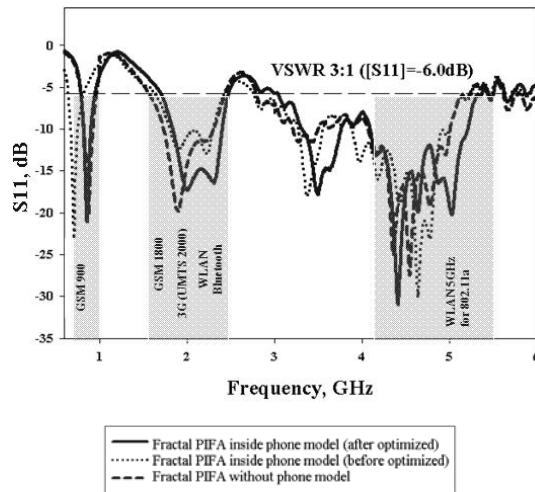The three-dimensional radiation patterns indicated the electric

**Figure 7.** F-PIFA S_{11} result.

field strength coverage of the antenna from all directions around the antenna; it must be considered that an antenna used for mobile applications cannot be guaranteed to be positioned in a particular orientation. With mobile application, the antenna is expected to operate in cluttered mobile environments where signal polarization is frequently randomized by reflections. Therefore, the performance of antennas in terms of both polarizations (i.e., the E-plane and H-plane polarization) was considered.

The planar antenna at the first and second resonant frequency has an almost omni directional while the E-plane is linear. However, when the planar antenna was operating at the third frequency, the polarization is directive. Therefore, the gain at this resonant is slightly high compare to the first and the second resonant because the antenna become more directive. However, the pattern shows almost omni directional radiation pattern. Consequently, it can be concluded that polarization performance of the planar antenna worsen as the resonant frequency is increased. Overall, however, the results were quite impressive and indicated that the planar antenna is well suited to mobile applications.

Omni-directional antennas propagate frequency signals in all directions equally on a horizontal plane but have limited range on the vertical plane. This radiation pattern resembles that of a very large doughnut with the antenna at the center of the hole. Omni-directional antennas provide the widest coverage, making it possible to form circular overlapping cells from multiple access points located throughout the building. Most access points that used standard Omni directional antennas having relatively low gain, around 2 to 4 dB. Hence, greater number of access points needed to cover specific area compares to higher gain.

(a)   (b)
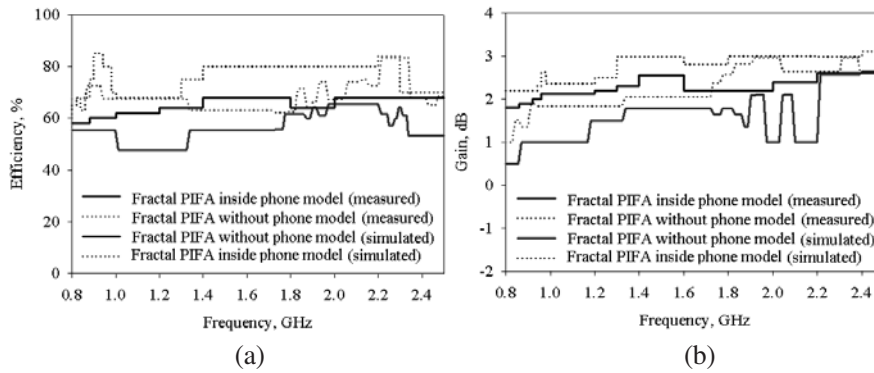
Figure 8. (a) Efficiency's result, (b) Gain's result.

(a)

(b)   (c)
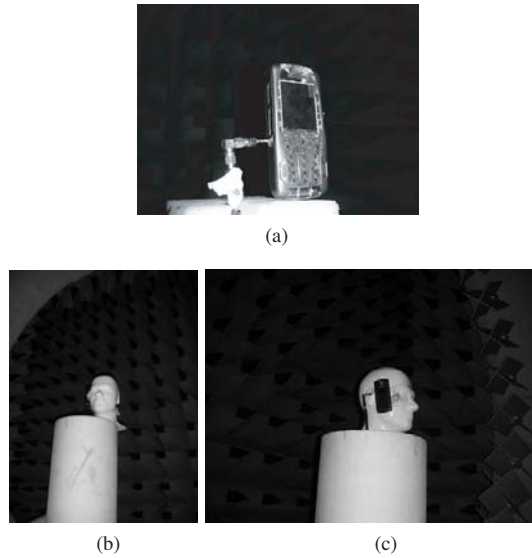
Figure 9. Position of the antenna during measurement in anechoic chamber.

4.2. Human Absorption of Radiation

A final test for mobile phone is to evaluate it in the presence of a human body with particular emphasis on the human head. Radio-frequency electrical currents in the antenna and in the housing of a handheld mobile phone will induce RF electric fields in tissue. As a result of this a part of the radiated energy will be absorbed into tissue causing an increase in the tissue temperature. The absorption is caused by the power loss involved with dielectric polarization. Vibrations of water molecules, movements of free ions and movements of bound charges attached to macro-molecules contribute most to the dielectric polarization in biological material in radio frequencies.

The SAR, used in the assessment of mobile phones, is a measure of the amount of EM (ElectroMagnetic) energy absorbed by biological tissue. The SAR is obtained by measuring the electric field in the simulated human tissues in close proximity to the device and is calculated by the formula (12) [24, 25].

$$\text{SAR} = \frac{\sigma}{\rho}\,|E|^2 = \frac{J^2}{\rho\sigma}\,[\text{W/kg}] \tag{12}$$

E: rms value of the electric field strength in the tissue [V/m];

J: Current density [A/m];

σ: conductivity of body tissue [S/m];

ρ: density of body tissues [kg/m^3]

The human head data consists of the types of tissues using Tissue Dielectric Properties program provided by FCC (Federal Communications Commission) [25, 26]. Table 5 shows the electrical properties of the brain and in Table 6 contain the SAR result at different operating frequencies.

SAR depends on the frequency operation, antenna type and distance between the antenna and the human body. As for this experiment, the antenna is placed 0.5 mm away from the SAM phantom and calculated over 10 g of the human tissue mass. SAR increases as the frequency of operation tends to higher frequency and this is due to the penetration depth and the fact at higher frequencies the power is absorbed more on the surface.

Base on radiation pattern result Figure 10 shows the PIFA radiation plot showing high Front to Back Ratio, which means a low SAR value. According to Swiss Regulation, the international SAR limit recommended for mobile phones is 2.0 watts per kilogram (W/kg) over ten grams of tissue. For United State government, they required the SAR level at or below 1.6 watts per kilogram (W/kg) taken over a
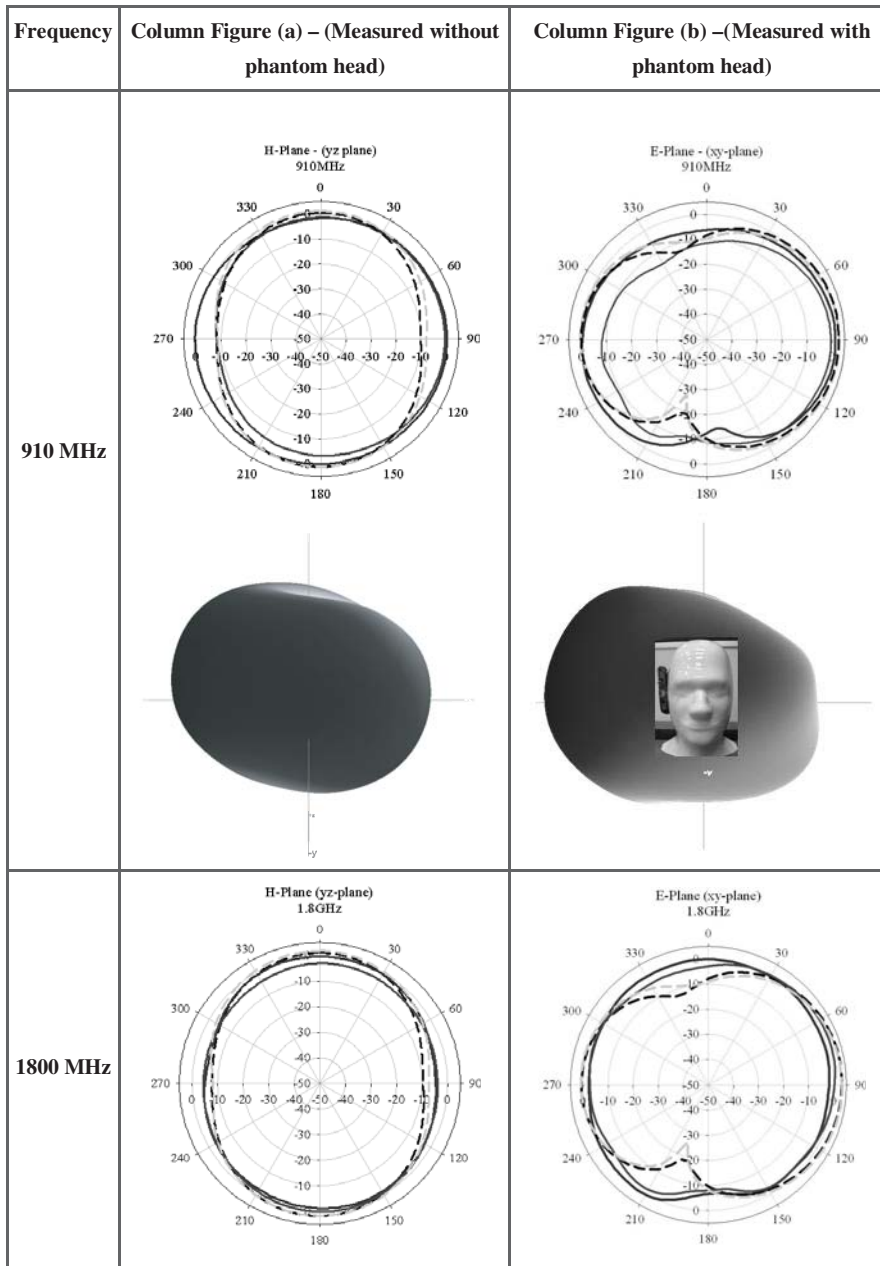
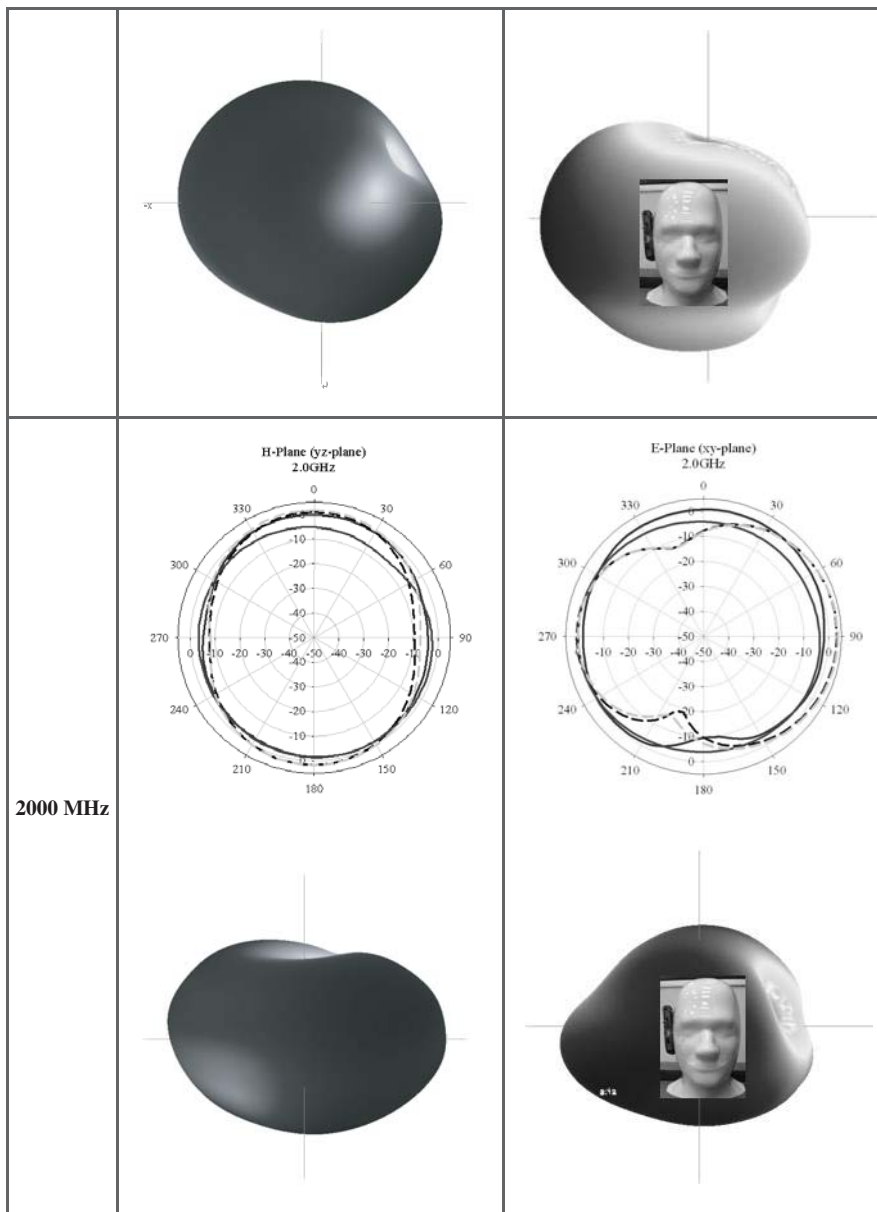**Table 5.** Material parameters for the SAM phantom.

Sam Material	Frequency [GHz]	Relative Permittivity (ε_r)	Conductivity [S/m]	Density [kg/m^3]
SAM Liquid	2.0	40.0	1.40	1000
SAM shell		3.5	0	1000

Table 6. SAR result at different operating frequency.

Freq (GHz)	SAR
0.9	0.255
2	0.817
1.6	0.996
2.5	1.08
4.8	1.47
5	1.55
5.8	1.59

Frequency	Column Figure (a) – (Measured without phantom head)	Column Figure (b) –(Measured with phantom head)
910 MHz		
1800 MHz		

H-Plane (yz-plane) 2.0GHz

**E-Plane (xy-plane) 2.0GHz**

2000 MHz
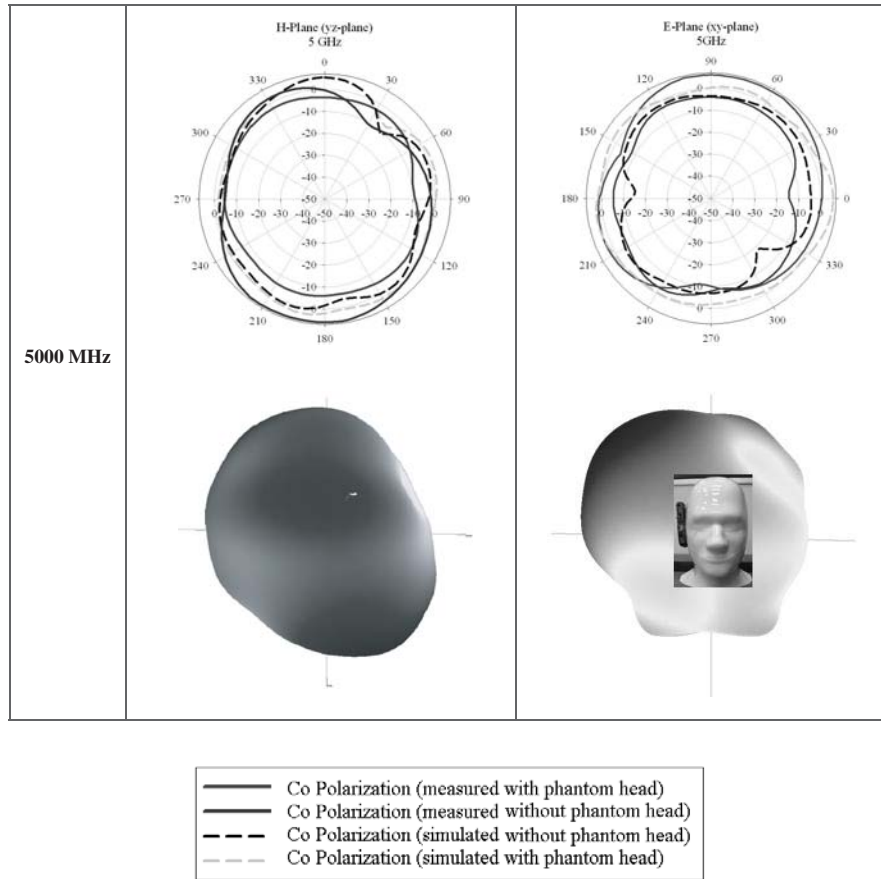
Figure 10. 2D and 3D radiation pattern of F-PIFA. (a) 3D radiation pattern without phantom head, (b) 3D radiation pattern with phantom head.

volume of 1 gram of tissue. As shown in Figure 11, indicates the value of the maximum SAR that had been calculated using CST software which is 1.59 W/kg.

The actual SAR level of an operating device can be below the maximum value because the device is designed to use only the power required to reach the network. That amount changes depending on number factors such as how close the user to a network base station. Use of devices accessories and enhancements may result in different SAR values. SAR values may vary depending on national reporting and testing requirement and the network band. Additional SAR information may be provided under product information at [25, 26].

```
Type       = SAR (rms)
Monitor    = loss (f=5.8) [1] (10g)
Maximum-3d = 1.59 W/kg
```
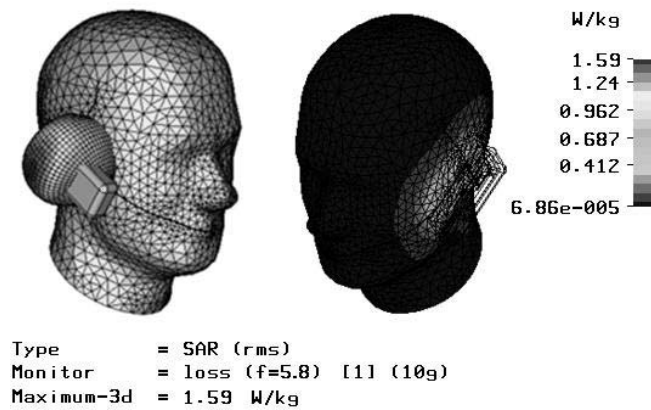
Figure 11. SAR calculation is done using CST simulation tools.

5. SUMMARY

The presented PIFA antenna covers the required operating frequency range for mobile phone application which are GSM 900, 1800, UMTS (Universal Mobile Telecommunication System), WLAN and HiperLAN (HigH Performance Radio LAN). An additional strip of copper is added to induce the F-PIFA current, creating the low resonant for GSM900. This antenna has been tested using mobile phone and the radiation patterns, gain and efficiency were measured in an anechoic chamber. It is observed that the radiation pattern in the two planes is omni-directional, thus, this antenna extremely suitable for applications in mobile communication devices. Its sensitivity to both the vertical and horizontal polarization is of immense practical importance in mobile cellular communication application because the antenna orientation is not fixed. This satisfies the requirements in wireless communication. Furthermore, the radiation pattern result showing high front to back ratio, meaning the antenna produce a low SAR value.

REFERENCES

1. da Silva, M. M., A. M. C. Correia, and R. Dinis, "Wireless systems on transmission techniques for multi-antenna W-CDMA system," *European Transactions on Telecommunications*, Vol. 20, No. 1, 107–121, Jan. 2009.

2. Balanis, C. A., *Antenna Theory: Analysis and Design*, 2nd edition, Wiley, New York, 1997.

3. Kraus, J. D. and R. J. Marhefka, *Antennas for All Applications*, 3rd edition, McGraw-Hill, Boston, 2002.

4. Waterhouse, R. B., *Microstrip Patch Antenna*, Kluwer Academic Publishers, Boston, 2003.

5. Garg, R., P. Bhartia, I. Bahl, and A. Ittipiboon, *Microstrip Antenna Design Handbook*, Artech House, Boston, 2001.

6. Werner, D. H., R. L. Haupt, and P. L. Werner, "Fractal antenna engineering: The theory and design of fractal antenna arrays," *IEEE Antennas and Propagation Magazine*, Vol. 41, No. 5, 37–59, Oct. 1999.

7. Guterman, J., A. A. Moreira, and C. Peixeiro, "Triple band miniaturized fractal planar inverted F-antenna for a small mobile terminal," *IEEE Transactions on Antennas and Propagation*, Vol. 1, 359–362, 2004.

8. Salonen, P., M. Keskilammi, and M. Kivikoski, "Single-feed dual-band planar inverted-F antenna with U-shaped slot," *IEEE Transactions on Antennas and Propagation*, Vol. 48, No. 8, 1262–1264, Aug. 2000.

9. Shin, Y.-S. and S.-O. Park, *A Novel Compact PIFA for Wireless Communication Applications*, 1–3, Conference Publication, Oct. 30–Nov. 2, 2007.

10. Geyi, W., Q. Rao, S. Ali, and D. Wang, "Handset antenna design: Practice and theory," *Progress In Electromagnetics Research*, PIER 80, 123–160, 2008.

11. Delaune, D., N. Guan, and K. Ito, "Simple multiband antenna for mobile phone application based on a dual-arm monopole structure," *PIERS Online*, Vol. 4, No. 1, 2008.

12. Hee, T. W., P. S. Hall, and C. T. Song, "Fractal PIFA, dipole and monopole antennas," *IEEE Topical Conference on Wireless Communication Technology*, 275–276, 2003.

13. Fuhl, J., P. Nowak, and E. Bonek, "Improved internal antenna for hand-held terminals," *Electron. Lett.*, Vol. 30, No. 22, 1816–1818, 1994.

14. Ebrahimi-Ganjeh, M. A. and A. R. Attari, "Interaction of dual band helical and PIFA handset antennas with human head and hand," *Progress In Electromagnetics Research*, PIER 77, 225–242, 2007.

15. Khalatbari, S., D. Sardari, A. A. Mirzaee, and H. A. Sadafi, "Calculating SAR in two models of the human head exposed to

mobile phones radiations at 900 and 1800 MHz," *PIERS Online*, Vol. 2, No. 1, 104–109, 2006.

16. Zhu, Y., F. Gao, X. Yang, H. Shen, W. Liu, H. Chen, and X. Jiang, "The effect of microwave emmision from mobile phones on neuron survival in rat central nervous system," *Progress In Electromagnetics Research*, PIER 82, 287–298, 2007.

17. Choi, D., C. Shin, N. Kim, and H. Shin, "Design and SAR analysis of broadband PIFA with triple band," *PIERS Online*, Vol. 1, No. 3, 290–293, 2005.

18. Hirata, A., K. Shirai, and O. Fujiwara, "On averaging mass of SAR correlating with temperature elevation due to a dipole antenna," *Progress In Electromagnetics Research*, PIER 84, 221–237, 2008.

19. Puente, C., J. Romeu, and A. Cardama, *Fractal-shaped Antennas, in Frontiers in Electromagnetics*, D. H. Werner and R. Mittra (eds.), IEEE Press, 2000.

20. Gianvittorio, J. and Y. A. Rahmat-Samii, "Fractal antennas: A novel antenna miniaturization technique, and applications," *IEEE, Antennas and Propagation Magazine*, Vol. 44, No. 1, 20–36, Feb. 2002.

21. Saidatul, N. A., A. A. H. Azremi, and P. J. Soh, "Analysis, design and fabrication of a hexagonal fractal antenna for multi-band applications," *International Conference on Intelligent and Advanced Systems (ICIAS'07)*, Kuala Lumpur, Nov. 25th–28th, 2007.

22. Guo, Y.-X., I. Ang, and M. Y. W. Chia, "Compact internal multiband antennas for mobile handsets," *Antennas and Wireless Propagation Letters, IEEE*, Vol. 2, 143–146, 2003.

23. Wong, K.-L., G.-Y. Lee, and T.-W. Chiou, "A low-profile planar monopole antenna for multiband operation of mobile handsets," *IEEE Transactions on Antennas and Propagation*, Vol. 51, 121–125, Jan. 1, 2003.

24. Kim, J.-H., Y.-H. You, K.-I. Lee, and J.-H. Yi, "Pilot-less synchronization receiver for UWB-based wireless application," *Progress In Electromagnetics Research*, PIER 83, 119–131, 2008.

25. Khalatbari, S., D. Sardari, A. A. Mirzaee, and H. A. Sadafi, "Calculating SAR in two models of the human head exposed to mobile phones radiations at 900 and 1800 MHz," *PIERS Online*, Vol. 2, No. 1, 104–109, 2006.

26. Choi, D., C. Shin, N. Kim, and H. Shin, "Design and SAR analysis of broadband PIFA with triple band," *PIERS Online*, Vol. 1, No. 3, 290–293, 2005.